Proc. Natl. Acad. Sci. USA
Vol. 73, No. 5, pp. 1384–1388, May 1976
Chemistry

Observation and interpretation of x-ray absorption edges in iron compounds and proteins

(metalloproteins/excited electronic states/x-ray absorption)

R. G. SHULMAN, Y. YAFET, P. EISENBERGER, AND W. E. BLUMBERG

Bell Laboratories, Murray Hill, New Jersey 07974

Contributed by R. G. Shulman, January 6, 1976

ABSTRACT **X-ray absorption spectra near the K_α edge have been measured in various iron group compounds using the intense synchrotron radiation available at the Stanford Synchrotron Research Project. In the cubic compounds KMF_3 where M = Mn^{+2}, Fe^{+2}, Co^{+2}, Ni^{+2}, and Zn^{+2}, well resolved lines were observed and assigned to the $1s \rightarrow 3d$, $1s \rightarrow 4s$, and $1s \rightarrow 4p$ transitions. The observed energies agreed rather well with the spectroscopic energy levels of the $Z+1$ ion and the intensities are shown to agree with those expected on the basis of one electron transitions of the form $Z\ 1s^2d^n(L,S) \rightarrow (Z+1)1s^2d^{n}n'l'(L'',S)$. The energies of the intense $1s \rightarrow 4p$ transition increase by about 5 V going from $KFeF_3$ to K_2NaFeF_6, but only by about 1 V from $K_4Fe(CN)_6$ to $K_3Fe(CN)_6$. The transitions confirm that upon oxidation of the hexacyanides the iron electronic structure barely changes. In the iron sulfur protein rubredoxin, where the iron is bound to a tetrahedron of sulfurs, the $1s \rightarrow 3d$ transition was about seven times more intense than the same transition in an octahedrally coordinated compound. These intensities parallel those observed in the d–d transitions of optical spectra, because in both types of spectra the intensities depend upon $4p$ admixture. In the heme protein cytochrome c, upon oxidation the $1s \rightarrow 4p$ transition shifts only about 1 V to higher energies, similar to the iron hexacyanides. These results are discussed in terms of covalent bonding.**

The absorption spectrum of x-rays near the K edge has traditionally been divided into a low energy region—the so-called absorption edge—in which the transitions are to bound states (1), and a higher energy region—the so-called extended x-ray absorption fine structure (EXAFS) spectrum—where the transitions are to free electron states (2–6). Recently, synchrotron sources of x-rays have become available whose intensities are about 10^5 times higher than were previously available. This results in improved signal to noise ratios, which allow meaningful measurements to be made on dilute systems (4–6).

In this paper we present measurements, made with synchrotron radiation, of the x-ray absorption spectrum of iron proteins, and of some model compounds in the region of the absorption edge. The model compounds which we have studied most intensively have been the extremely ionic fluorides, in order to facilitate the interpretation in terms of free ion states. Transitions from the $1s$ to the $3d$, $4s$, and $4p$ states, in the model compounds, have been assigned by comparing measured transition intensities and energies with quantitative theoretical calculations based on atomic states. This is an extension and refinement of the present qualitative understanding recently reviewed by Srivastana and Nigam (7). In this work the model systems are highly ionic, and the theoretical approach of using appropriate atomic levels as a starting point works very well. It is shown how these interpretations can be extended by molecular orbital calculations and the use of other experimental measurements which independently determine the charge of the ion. For metalloproteins, where the metal atom has strongly covalent bonds, an approach including these interactions will be required for an equally complete understanding. However, even without more quantitative studies of covalency, we show that one can presently arrive at interesting qualitative conclusions about the structure of metal ion sites in proteins and their electronic states.

Abbreviation: EXAFS, extended x-ray absorption fine structure.

RESULTS

For simplicity we first compare ferrous and ferric compounds where the irons are in sites of O_h symmetry, and where the surrounding regular octahedra are fluoride ions (Fig. 1). We note that the first indications of absorption, in both compounds, are weak peaks which have been enlarged to facilitate comparison. The K_2NaFeF_6 peak is shifted about 1.3 V to higher energies from the analogous peak in $KFeF_3$. The K_2NaFeF_6 peak stands by itself and is composed of a barely resolved doublet. The $KFeF_3$ peak is less clearly separated from the base of the strong absorption, with the suggestion of a weaker peak about 2 V to higher energy.

About 16 V to higher energies in the ferrous compound, and 19 V to higher energy in the ferric compound, there is an intense peak whose position depends upon the oxidation state of the iron. At somewhat lower energies, there are shoulders on this intense peak of varying degrees of resolution.

We measured the absorption spectra of a series of perovskite cubic fluorides where the divalent metal ion changes from Mn^{+2} to Zn^{+2} with the results shown in Fig. 2. The first weak absorption is assigned to the $1s \rightarrow 3d$ transition since it is observed in all but $KZnF_3$ which has no empty $3d$ orbital. The second absorption, present either as a shoulder or a peak about 9 V higher, is the $1s \rightarrow 4s$ transition, and the intense absorption about 16 V above the first absorption is the $1s \rightarrow 4p$. These assignments are based upon the agreement between the calculated and measured values of the energies shown in Table 1 and the selection rules and intensities discussed in the next section.

Fig. 3 shows the kind of chemical information which we would like to obtain from x-ray absorption edge measurements, and at the same time illustrates the uncertainties which must first be understood. In the fluorides, theory and experiment have shown that about 90% of the formal change of charge of the $3d$ shell actually shows up as a real change of charge (8). By contrast, the iron atoms in the two hexacyanides were close to isoelectronic (9). In this respect, the hexacyanides are analogous to the heme compounds and proteins, where numerous investigations have suggested that the formal charge has little correlation with the actual charge on the iron atom (10).

Fig. 3 provides some support for these preconceptions. As seen in the analogous fluoride compounds in Fig. 1, the edge of the first strong absorption in FeF_3 is about 5 V higher than that of FeF_2. This reflects the greater energy required for removing the $1s$ electron to an outer state in the ferric compound.

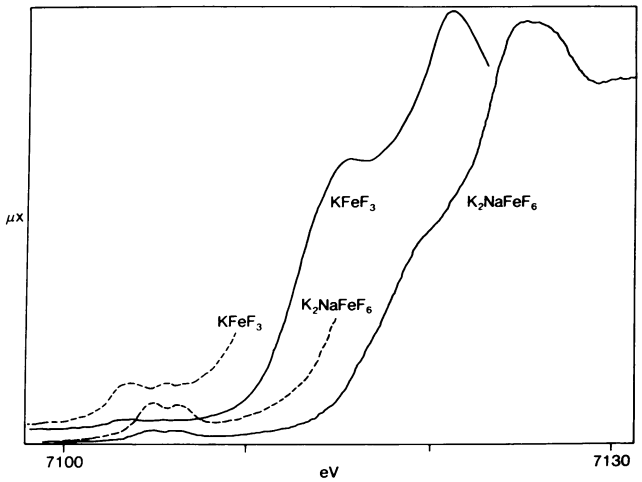

FIG. 1. The x-ray absorption spectra of $KFeF_3$ and K_2NaFeF_6. The incomplete dashed and solid curves are the $KFeF_3$ and K_2NaFeF_6 absorptions multiplied by 4 and 5, respectively. All measurements made on powdered samples at 300 K.

In the hexacyanides, the two absorptions are separated by only about 1 V over the entire edge, and the absorptions reflect the similar electronic structures of the metal atom.

An illustration of the information available from the edge position in proteins is given in Fig. 4. Formally reducing cytochrome *c* at pH 7 shifts the $1s \rightarrow 4p$ transition about 1 V to lower energies. By contrast, if the sixth ligand, which is methionine at pH 7, is changed to the amino group of a lysine side chain at pH >10.5, then the $1s \rightarrow 4p$ peak and edge shift by about 2 V to higher energies.

Another informative aspect of the edge spectra is illustrated in Fig. 5 by two iron–sulfur complexes. In the protein rubredoxin, the ferric iron is known to be tetrahedrally coordinated to four sulfurs of cysteinyl side chains (11, 12). In the model compound tris(pyrrolidine carbodithioate-*S*,*S*′) iron(III), symbolized by FESSC, the ferric iron is octahedrally coordinated to six sulfurs (13). The $1s \rightarrow 3d$ to $1s \rightarrow 4p$ intensity ratio is seven times larger in the tetrahedral coordination than in octahedral. The explanation given below shows how the intensity of the $1s \rightarrow 3d$ transition of iron group ions can be used as an indicator of their site symmetry.

DISCUSSION

We first discuss these observations in terms of atomic levels which are most relevant to the very ionic compounds, particularly in the energy region within 40 eV of the absorption threshold. Because the binding energies of the 1*s* levels in the ion group are several keV, correlation effects are completely negligible and the transitions are one-electron in character, i.e.,

$$[1s^2 2s^2 2p^6 3s^2 3p^6]3d^n(L,S) \longrightarrow [1s2s^2 2p^6 3s^2 3p^6]3d^n,n'l'(L'',S), \quad [1]$$

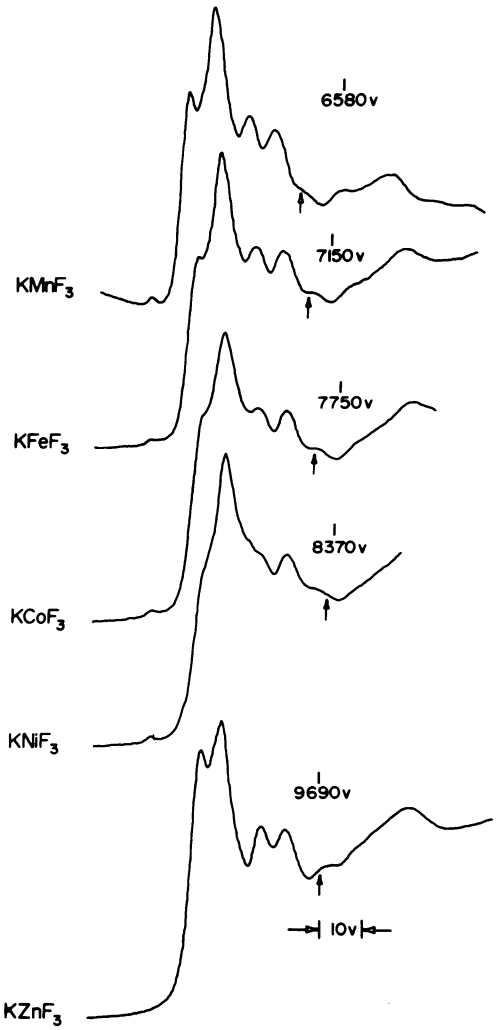

FIG. 2. X-ray absorption of the KXF_3 perovskite cubic series. Each spectrum covers a different energy range as indicated, but the energy intervals are all given by the 10 V marker. The arrows show the position of the spectroscopic ionization potential, measured from the 4*p* level.

where the orbital quantum number *L* changes in the transition but the spin quantum number *S* does not. The electronic configurations enclosed in brackets represent the core of the ion, and include relaxation in the final state. In the present treatment, it is assumed that the excited one-electron state $n'l'$ is atomic in character and localized on the metal ion.

To classify the final states of the ion in more detail, we note that the multiplet state of the unfilled *d* shell, $d^n(L,S)$ does not change in the transition. This is obvious since the transitions are for a single electron, but a formal proof can also be obtained by the methods of atomic spectroscopy (14). Furthermore, because

Table 1. Comparison of experimental and theoretical orbital transitions

Salt	$3d-4s$, experimental/theoretical	$3d-4p$, experimental/theoretical	$4s-4p$, experimental/theoretical	$4p-5p$, experimental/theoretical
$KMnF_3$	7.6/4.3	14.3/10.6	6.7/6.3	8.1/10.2
$KFeF_3$	9.7/6.4	15.8/13.0	6.1/6.6	8.2/—
$KCoF_3$	10.5/7.1	16.7/14.3	6.2/7.1	8.2/—
$KNiF_3$	11.0/8.0	17.3/15.3	6.3/7.3	7.5/—
$KZnF_3$			5.3/8.2	9.0/11.8
K_2NaFeF_6	12.0/13	19/23	7/10	

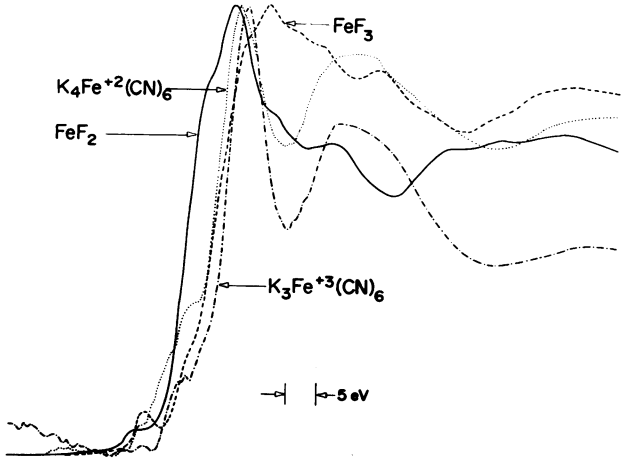

FIG. 3. The edge absorption in the iron fluorides and hexacyanides in the region near the iron K_α edge.

the 1*s* hole is so close to the nucleus, as far as the energetics of the outer shells is concerned the final state of an ion having atomic number Z can be taken as that of an ion with atomic number Z + 1, but having a fully occupied 1*s* shell. This enables us to use the spectroscopic tables of the element (Z + 1) to describe the energies of the fully relaxed ion. In principle, the final state $3d^n n'l'$ is coupled to the spin of the remaining 1*s* electron. However, the 1*s* to 3*d* exchange interaction is completely negligible. In summary, the presence of the 1*s* hole in the final state is neglected except insofar as it leads to a core electronic rearrangement. For example, the final state of the K transition of $Fe^{+2}(d^6)$ is taken as $Co^{+2}(d^6,n'l')$. A general description of the final state of the excited ion of atomic number Z, neglecting exchange with the 1*s* hole, is therefore

$$(Z + 1)[1s^2,2s^2,2p^6,3s^2,3p^6]3d^n(LS),n'l'(L'',S''), \quad [2]$$

where $S'' = S \pm \frac{1}{2}$. From Eq. 5.17 of reference (14), it is seen that the statistical weights of transitions to the substates of L'', S'' are proportional to $(2L'' + 1)(2S'' + 1)$. It is possible then, by knowing which $(n'l')$ values are allowed by the symmetry of the transition operator, to predict the structure of the absorption spectrum by reference to atomic tables.

The spectra of Figs. 1–3 show that transition metal ions have a very weak absorption peak at threshold, followed by a shoulder on a rising absorption curve which culminates in a strong peak. We identify this strong peak as the allowed transition 1*s* $\rightarrow$4*p*, the lower energy shoulder as the forbidden transition 1*s* $\rightarrow$4*s*, and the small peak at threshold as the forbidden transition 1*s* $\rightarrow$3*d*. The energy separations between these assigned transitions correspond to the spectroscopic values, in the appropriate free ions, as shown in Table 1. The experimental values of the 3*d*–4*s* splittings increase by about 3.5 V from $KMnF_3$ to $KZnF_3$, as do the free ions' values. Note that free ion spectroscopic values (15) are consistently about 3 V less than the observed splittings. Similar trends and constant differences are seen in the 3*d*–4*p* splittings, with the result that experimental and free ion values of the 4*s*–4*p* splitting are in approximate agreement.

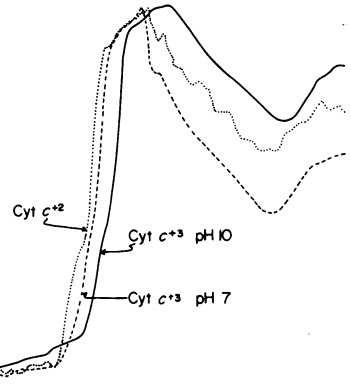

FIG. 4. Comparison of the absorption edges in horse heart cytochrome *c* comparing the shift observed by a rise in the pH with the smaller shift observed upon oxidation.

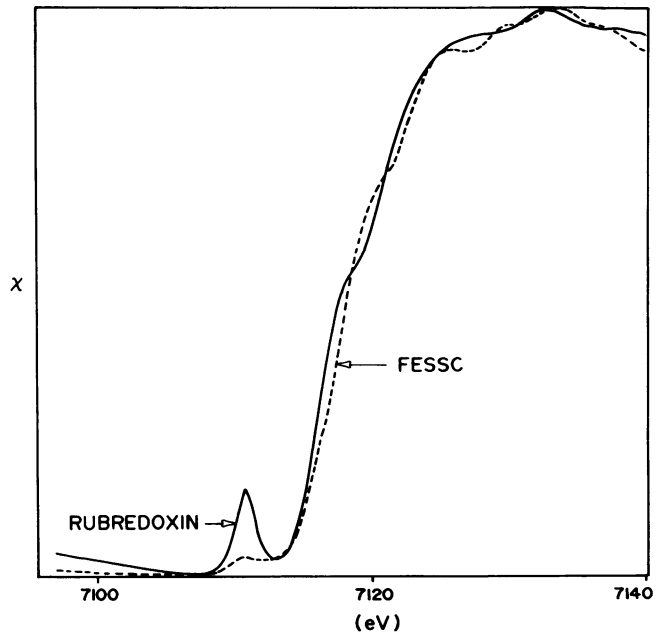

FIG. 5. Absorption of the tetrahedrally coordinated iron in rubredoxin *P. aerogenes* and of the octahedrally coordinated iron in tris(pyrrolidine carbodithioate-*S*,*S'*) iron(III). The major difference is in the intensity of the lowest energy absorption which is several times more intense in rubredoxin. Although the relative energy scales are accurate to within ±0.5 V, the absolute scale may be in error by one volt.

A comparison of observed and free ion splittings in K_2NaFeF_6 is given in the last line of the table. Free ion values, which could not be obtained from spectroscopic tables, were obtained from calculations by Noorman and Schrijver (16). It can be seen from the table that the 3*d* position moves about 1 V to higher energy going from ferrous to ferric and that the 3*d* $\rightarrow$4*p* splitting increases by about 4 V, the same as were observed between FeF_2 and FeF_3.

We now consider the fact that in 1*s* $\rightarrow$3*d* transitions the final Z + 1, $(3d)^{n+1}$ configuration has a multiplet structure. In the cases of $KMnF_3$, $KFeF_3$, $KCoF_3$, and $KNiF_3$, the final states d^{n+1} are, respectively, those of Fe^{+2}, d^6; Co^{+2}, d^7; Ni^{+2}, d^8; and Cu^{+2}, d^9. Keeping in mind that the initial states of all the ions are those of maximum spin multiplicity, two final states can be reached in the cases of $KFeF_3$ and $KCoF_3$, namely, ^4F and ^4P for $KFeF_3$ and ^3F and ^3P for $KCoF_3$. In both cases, the F to P energy separation is about 2 eV (15), the F level being the lower. We have calculated the relative intensities of these two forbidden transitions under the assumption that the *p*–*d* mixing is due to an interaction which transforms like the set (*x*,*y*,*z*). The results are that the intensities are proportional to $(2L'' + 1)$, i.e., in the ratio 7 to 3 for the F and P states, respectively. We expect, then, a weaker absorption about 2 eV above the lowest 1*s* $\rightarrow$ 3*d* transition in the cases of $KFeF_3$ and $KCoF_3$, but not for $KMnF_3$ or $KNiF_3$. Examination of the spectra in

Figs. 1 and 3 shows that there are minima from the $1s \rightarrow 3d$ absorption in $KMnF_3$ and $KNiF_3$ but not in $KFeF_3$ and $KCoF_3$, exactly as predicted.

The splitting of 1.5 eV in the $1s \rightarrow 3d$ transition of K_2NaFeF_6 (see Fig. 1) is caused by crystal field splitting of the ground state. This agrees with the crystal field splitting of cobaltic fluorides observed by optical spectroscopy which are about 1.4 to 1.6 eV (17). It is clear, furthermore, that the crystal field splitting would not be observable in the divalent fluorides because optical crystal field splittings are about 1 eV and the natural linewidths of the x-ray absorption spectra are about 1.5 eV. Static Jahn–Teller distortions of the excited state can be disregarded, because similar splittings are observed in FeF_3 and cubic K_2NaFeF_6. Dynamic Jahn–Teller distortions of cobaltic fluorides have been shown to be about ½ eV, which are negligible compared to the observed splittings (17).

The ratio of the areas under the weak peak at threshold assigned to $1s \rightarrow 3d$ and the strong peak assigned to the $1s \rightarrow 4p$ transition gives a value of about 4×10^{-3}. Two possible sources of the $1s \rightarrow 3d$ intensities are quadrupole transitions and $3d$–$4p$ mixing due to vibronic interactions. We have estimated that the quadrupole transitions are three orders of magnitude weaker than those observed. This leaves the even–odd orbital mixing due to vibronic interactions as the likely origin of the intensity, which has previously been shown to be the mechanism responsible for the optical transitions in these ions (18). Optical transitions of octahedral centrosymmetric complexes of Ni^{+2} and Co^{+2} in the $KMgF_3$ host crystal have measured intensities, at liquid helium temperatures, about 10^{-4} times as strong as the parity allowed $3d \rightarrow 4p$ transitions (19). This ratio would be increased a factor of two to three at 300 K and would be increased by another factor of about three when the sum is taken over all states of the d manifold. Hence, within experimental and theoretical uncertainties, the intensities observed for the $1s \rightarrow 3d$ transitions are in agreement with the expectations from optical spectroscopy. The $1s \rightarrow 4s$ transitions are considerably more intense than the $1s \rightarrow 3d$, approximately by a factor of 10. This is to be expected if they are also due to vibronic mixing, because the energy separation between the $4s$ and $4p$ levels, as observed on the spectra, is about ⅓ of the separation between the $3d$ and $4p$ level. Since the energy denominator occurs squared in the transition rate, a ratio of about 10 for the corresponding intensities would be expected.

The $1s \rightarrow 3d$ absorption in the molecule rubredoxin, where Fe^{+3} is tetrahedrally coordinated to four sulfur atoms, is seen (Fig. 5) to be considerably more intense than in the octahedral FESSC, which has a center of inversion. Since there is no inversion center in tetrahedral coordination, the $3d$–$4p$ mixing is stronger than in octahedral symmetry, as is well known from optical spectroscopy (18), and experimental results have shown that the forbidden transitions should be 10 to 100 times stronger than in octahedral symmetry (20). The observed intensity ratio is about seven which, while smaller, is in the right direction.

There exists the possibility of transitions to higher p states, i.e., $n' > 4$. The close numerical agreements in the table between the observed intervals from the $4p$ peaks to the next higher energy peak, and the spectroscopic $4p$–$5p$ splitting, suggest this assignment. The radius of a hydrogenic $n'p$ orbital in a nuclear charge of +3 is $(n'/3)a_0$. The distance of the F^- site to the metal ion is 2.1 Å and the radius of the F^- ion is 1.36 Å. Hence, the maximum of the $4p$ orbital is well within the cavity formed by the six F^- ions. For the $5p$ orbital, however, the maximum falls at the edge of the F^- ion, so that the limitations of the atomic model must be explored before this assignment can be confirmed. Spectroscopic values of the interval between the $4p$ levels and the ionization potentials are indicated by the arrows in Fig. 2. Because the Madelung potential at the metal ion site will always make it easier to free an electron, no localized ionic features can exist at energies higher than the arrows. These considerations lead us to suggest that the zero of energy for the EXAFS region should be fixed at 5–10 V above the $4p$ level.

It is clear from the present results that both $4s$ and $4p$ final states are raised by interactions with the fluoride environment, hence these states, in a molecular orbital picture, are antibonding, which is consistent with bonding to lower fluoride orbitals. Previous molecular orbital calculations (21) of the bonding in $KNiF_3$ have shown that unperturbed energies of the F^-2p orbitals were about 7 eV lower than the $3d$ levels of Ni^{+2}. The low ionization potential of F^- (about 5 eV) means that all higher empty F^- orbitals (i.e., $3p$, $4p$, etc.) will be considerably below the metal $4s$ or $4p$ orbitals; so that in the present bonding interaction it is to be expected that the final states with appreciable iron character will be raised in energy as is observed.

In the ionic fluorides the $1s$–$4p$ transition moves about 5 eV to higher energy going from ferrous to ferric. Before discussing the effects responsible for these shifts, it is important to note just which experimental features are being discussed. The shape of the low energy side of the intense $1s$–$4p$ transition is determined by the contribution from lower energy, lower intensity transitions, such as the $1s$–$4s$. In solution complexes of $(FeF_6)^{-3}$ the $1s$–$4s$ transition cannot be seen, presumably because of weaker vibronic mixing, while the $1s$–$3d$ and $1s$–$4p$ transitions coincide perfectly with those observed for $(FeF_6)^{-3}$ complexes in a K_2NaFeF_6 crystal (Shulman and Eisenberger, to be published). This change in $1s$–$4s$ intensity introduces an apparent edge shift of several volts which should not be taken as an indicator of the $1s$–$4p$ energy. Since in general the low energy shoulder has contributions from perturbations of otherwise forbidden transitions, we suggest that the peaks rather than the edges be used as indicators of the transition energy. In this respect, it should be noted that Cotton and Hanson (22) assigned the splittings, between the transitions we identify as $1s$–$4s$ and $1s$–$4p$, to a crystal field splitting of the $4p$ level. On this basis, however, they were not able to account for the splittings observed in cubic compounds, such as are shown in Fig. 2 which *are* explained by the present analysis.

Considering the energy of the state associated with the ionic $4p$ state, in terms of the contribution from charge and covalency, we note that it will increase when the covalency increases, if, as assumed above for the fluorides, it is an antibonding state. Second, it will increase as the charge of the metal ion increases, since the virial theorem states that the potential energy always dominates, so that as the core attraction increases it becomes harder to promote an electron from $1s \rightarrow 4p$. The energy of the transition from $1s$ to antibonding $4p$ states is described by perturbation theory in a molecular orbital approach as

$$\epsilon_{1s\text{-}4p^*} = \epsilon_{4p}(p) + \frac{h_{ij}^2}{h_{ii} - h_{jj}} - \epsilon_{1s} \qquad [3]$$

where $\epsilon_{4p}(q)$ is the energy of the ionic $4p$ level which is a function of charge q. The second term is the increase of this energy by the covalent interaction, h_{ij} being the off diagonal matrix element and h_{ii} and h_{jj} the two diagonal matrix elements, while ϵ_{1s} is assumed to be independent of charge. Since increasing positive charge increases the first term in Eq. 3, and increasing covalency by definition increases the second, it is clear that as the covalency is increased these terms will either reinforce each other (for electron donation to the ligands) or tend to cancel (for electron donation to the metal). Since the

measured $1s$–$4p^*$ energy is a single parameter, we cannot determine the separate contributions of the two terms in Eq. 3 without additional information. The small shift observed in the hexacyanides means that the sum of the first and second terms in Eq. 3 does not change upon oxidation. The previous analysis of Mössbauer isomer shifts and ESR data suggested (9) that the iron did not change its charge upon oxidation. Consequently the very small shifts in the $1s \rightarrow 4p^*$ energies (Fig. 3) show that neither the charge nor the covalency change appreciably. While the energy of the transition is the more meaningful property, we have discussed it in terms of covalency and charge in accordance with the established chemical approach.

A similar analysis of our cytochrome *c* data is beyond the scope of the present study, because the complementary properties such as the Mössbauer isomer shifts and ESR g tensors have not been analyzed in terms of the electronic state of the iron. The simplest explanation is that cytochrome *c* acts like the hexacyanides in that the electronic state of the iron does not change upon oxidation, which is consistent with the negligible $1s \rightarrow 4p^*$ shift observed. The large shift to higher energies, observed after a rise in the pH of ferricytochrome *c* and, thereby, a replacement of the sulfur ligand by a nitrogen, comes from a change in the electronic state. Presumably this includes contributions from the iron which becomes more positive, as would be expected from the relative electron donating tendencies of nitrogen and sulfur. Clearly, correlations between the x-ray absorption measurements and other data can be used to delineate the details of the bonds in the terms used above. Another important feature of the x-ray absorption measurements is that they determine energies of virtual states, i.e., excited states of the Z + 1 complex such as would be calculated by a molecular Hartree–Fock solution. The observed transition energies for a complex with metal ion, Z, can be directly compared with the results of molecular orbital calculations, made for the complex with metal ion Z + 1 at the internuclear distances characteristic of the Z complex.

We thank H. J. Guggenheim for several samples and P. H. Citrin, J. J. Hopfield, P. A. Lee, B. K. Teo, and G. K. Wertheim for helpful conversations. This work was performed at the Stanford Synchrotron Radiation Facility which is supported by National Science Foundation Grant no. DMR73-07692 in cooperation with the Stanford Linear Accelerator and the U.S. Energy Research and Development Administration.

1. Kossel, W. (1920) Z. *Phys.* **1**, 119–134.
2. de L. Kronig, R. (1931) *Physik* **70**, 317–323.
3. Sayers, D., Lytle, F. & Stern, E. A. (1970) in *Advances in X-Ray Analysis* (Plenum Press, New York), Vol. 13, p. 248.
4. Kincaid, B. M. & Eisenberger, P. (1975) *Phys. Rev. Lett.* **34**, 1361–1364.
5. Kincaid, B. M., Eisenberger, P. & Sayers, D. (1975) *Phys. Rev.*, in press.
6. Shulman, R. G., Eisenberger, P., Blumberg, W. E. & Stombaugh, N. A. (1975) *Proc. Natl. Acad. Sci. USA* **72**, 4003–4007.
7. Srivastava, U. C. & Nigam, H. L. (1972–1973) *Coord. Chem. Rev.* **9**, 275–310.
8. Shulman, R. G. & Sugano, S. (1963) *Phys. Rev.* **130**, 506–511.
9. Shulman, R. G. & Sugano, S. (1965) *J. Chem. Phys.* **42**, 39–43.
10. Zerner, M., Gouterman, M. & Kobayashi, H. (1966) *Theor. Chim. Acta* **6**, 363–400.
11. Bachmayer, H., Piette, L. H., Yasunobu, K. T. & Whiteley, H. R. (1967) *Proc. Natl. Acad. Sci. USA* **57**, 122–127.
12. Watenpaugh, K. D., Sieker, L. C., Herriott, J. R. & Jensen, J. H. (1973) *Acta Crystallogr. Sect. B* **29**, 943–956.
13. Healy, P. C. & White, A. H. (1972) *J. Chem. Soc. Dalton Trans.* 1163–1171.
14. Shore, B. W. & Menzel, D. H. (1968) *Principles of Atomic Spectra* (J. Wiley & Sons, New York).
15. Moore, C. E. (1952) "Atomic energy levels," *Nat. Bur. Stand. (U.S.) Cir.* **467**, Vol. II, August 15, 1952.
16. Noorman, P. E. & Schrijver, J. (1967) *Physica* **36**, 547–556.
17. Cotton, F. A. & Meyers, M. D. (1960) *J. Am. Chem. Soc.* **82**, 5023–5026.
18. Ballhausen, C. J. (1962) in *Ligand Field Theory* (McGraw-Hill, New York), chap. 8.
19. Sugano, S., Tanabe, Y. & Kamimura, H. (1970) in *Multiplets of Transition-Metal Ions in Crystals* (Academic Press, New York), chap. 5.
20. Pappalardo, R., Wood, D. L. & Linares, R. C. (1961) *J. Chem. Phys.* **35**, 1460–1478.
21. Sugano, S. & Shulman, R. G. (1963) *Phys. Rev.* **130**, 517–530.
22. Cotton, F. A. & Hanson, H. P. (1958) *J. Chem. Phys.* **28**, 83–87.
23. Sugano, S., Tanabe, Y. & Kamimura, H. (1970) in *Multiplets of Transition-Metal Ions in Crystals* (Academic Press, New York), chap. 9.